**Proceedings of ASME Turbo Expo 2004:**
**Power for Land, Sea, and Air**
**June 14–17, 2004, Vienna, Austria**

# GT2004-53900

# COUPLING OF BIOMASS STEAM GASIFICATION AND AN SOFC - GAS TURBINE HYBRID SYSTEM FOR HIGHLY EFFICIENT ELECTRICITY GENERATION

**Tobias Proell**
Institute of Chemical Engineering
Vienna University of Technology
Getreidemarkt 9/166, 1060 Vienna, Austria
Phone: +43 1 58801 15965, Fax: +43 1 58801 15999
tproell@mail.zserv.tuwien.ac.at

**Reinhard Rauch**
Institute of Chemical Engineering
Vienna University of Technology
Getreidemarkt 9/166, 1060 Vienna, Austria
Phone: +43 1 58801 15954, Fax: +43 1 58801 15999
rrauch@mail.zserv.tuwien.ac.at

**Christian Aichernig**
Repotec Umwelttechnik GmbH
Europastrasse 1, 7540 Guessing, Austria
Phone: +43 1 216 18 95, Fax: +43 1 5852615 15
c.aichernig@repotec.at

**Hermann Hofbauer**
Institute of Chemical Engineering
Vienna University of Technology
Getreidemarkt 9/166, 1060 Vienna, Austria
Phone: +43 1 58801 15970, Fax: +43 1 58801 15999
hhofba@mail.zserv.tuwien.ac.at

## ABSTRACT

An energetic model of an internal reforming solid oxide fuel cell (IRSOFC) is developed. It is integrated in a process coupling fluidized bed steam gasification of biomass and an IRSOFC-gas turbine hybrid cycle. Process simulation is performed using the software package IPSEpro. The model of the gasification and gas conditioning section is based on data from the 8 MW (fuel power) plant in Guessing/Austria, while the fuel cell is modeled based on recent literature data. Heat utilization for power generation is considered covering both hybrid cycle exhaust and heat from the gasification process. Electric efficiencies up to 43 % are expected for combined heat and power application even at small plant capacities in the range of 8 MW fuel power.

Keywords: Biomass, Gasification, Solid oxide fuel cell, Hybrid system, Combined heat and power

## INTRODUCTION

Along with the present discussion about gradually substituting fossil fuels by sustainable sources, biomass gasification systems have been developed based on different approaches. In Austria, a dual fluidized bed gasification system has been developed using steam as the gasification agent and providing the necessary heat in the gasification reactor by circulating hot bed material [1]. It is heated up in a second fluidized bed reactor by combustion of residual char. An 8 MW (fuel power) demonstration plant [2] is operated in Guessing/Austria since December 2001 and reached 6500 hours of operation in November 2003. For power generation, a 2 $MW_{el}$ gas engine is used requiring a two step cold gas cleaning system consisting of a bag filter and an organic solvent scrubber for tar removal. The plant is operated in combined heat and power (CHP)-mode and reaches an electric efficiency of 25 % (gross) at a total fuel utilization of about 70 %. The steam gasification producer gas is – in contrast to the air gasification systems – almost free of inert nitrogen and shows lower heating values (LHV) between 12 and 14 $MJ/m^3_N$ (dry gas). The gas composition shown in Table 1 largely resembles the composition of partly reformed natural gas and the spectrum of possible gas application is considerably higher than for air gasification systems. The most prospective technologies to utilize the producer gas apart from "conventional" combustion in turbines or engines are high temperature fuel cells for electricity generation and syntheses – either of high quality liquid fuels or of synthetic natural gas.

Gas turbines (GT) have been discussed in combination with gasification of biomass for pressurized gasifiers and high temperature producer gas cleaning. However, continuous solid feed to the pressurized systems is still a key-problem. Another critical point is the availability of hot gas conditioning technologies in order to meet the gas turbine specifications for long-term operation. On the other hand, atmospheric gasification systems can produce fuel for internal combusting GT. Because of the need for fuel gas compression, the producer

gas must be cooled, what is usually done along with gas conditioning (cold gas cleaning). In this case, the GT is directly competing to gas engines, which are still advantageous with respect to gas cleanliness requirements and efficiency in the power range of 1-5 $MW_{el}$ [3], which is the typical size of biomass CHP-application.

**Table 1**
**Typical dry composition of producer gas from the Guessing steam gasification process**

| | | |
|---|---|---|
| $CH_4$ | v-% (dry) | 10…11 |
| $C_2H_4$ | v-% (dry) | 2…2.5 |
| $C_3$-Fract. | v-% (dry) | 0.5…0.7 |
| CO | v-% (dry) | 24…26 |
| $CO_2$ | v-% (dry) | 20…22 |
| $H_2$ | v-% (dry) | 38…40 |
| $N_2$ | v-% (dry) | 1.2…2.0 |
| LHV | $MJ/m^3_N$ (dry) | 12.9…13.6 |

Owing to the high hydrogen content and the potential of steam reforming for the hydrocarbon fraction, the steam gasification producer gas represents a fuel well adapted to the requirements of high temperature fuel cells. Recently, solid oxide fuel cell (SOFC)-GT hybrid concepts have been published for natural gas applications [4-10] and also in combination with biomass gasification [11]. SOFC stacks work in the temperature range from 800 to 1000 °C and the fuel cell performance ideally increases with increasing pressure [4]. Therefore, the SOFC represents a suitable topping cycle for external combusting GT-systems. The high operating temperature allows internal steam reforming of methane and CO-shifting at the anode surface, which guarantees high fuel conversion rates. Chan et al. [12] treat the energetic modeling of internal reforming SOFC (IRSOFC) into detail. The same authors present a fuel cell-GT hybrid system based on performance data of a tubular IRSOFC [8,9], on which the present work is largely based.

The Guessing steam gasification process including gas cleaning has been already modeled and implemented into the equation-oriented process simulation tool IPSEpro [3]. Within the present work, the simulation has been extended by the model of the IRSOFC stack and a coupling between the gasification process and an IRSOFC-GT hybrid concept is realized in the simulation program. A steam cycle and a compact organic Rankine cycle (ORC) are discussed as possible concepts for heat recovery across the plant.

## NOMENCLATURE

| | | |
|---|---|---|
| $A_{eff}$ | effective sectional area of the cell stack | $m^2$ |
| $E$ | electric potential of the fuel cell | V |
| $E_0$ | theoretic fue cell potential for lhv of $H_2$ | V |
| $E_{0i}$ | molar standard exergy of species i | $J \cdot mol^{-1}$ |
| $E_A$ | activation energy | $J \cdot mol^{-1}$ |
| $e$ | specific exergy of a stream | $J \cdot kg^{-1}$ |
| $F$ | Faraday constant ($F$ = 96485.3) | $A \cdot s \cdot mol^{-1}$ |
| $\Delta G_R^0$ | Gibbs free reaction enthalpy at 0.1 MPa | $J \cdot mol^{-1}$ |
| $\Delta_f H_{298}^0$ | standard enthalpy of formation | $J \cdot mol^{-1}$ |
| $h$ | specific enthalpy of a stream | $J \cdot kg^{-1}$ |
| $i$ | mean current density of the cell stack | $A \cdot m^{-2}$ |
| $i_0$ | exchange current density | $A \cdot m^{-2}$ |
| $i_L$ | limiting current density | $A \cdot m^{-2}$ |
| $L$ | total length of fuel cell channel | m |
| $LHV$ | molar lower heating value | $J \cdot mol^{-1}$ |
| $lhv$ | specific lower heating value | $J \cdot kg^{-1}$ |
| $M$ | mean molar mass of a stream | $kg \cdot mol^{-1}$ |
| $\dot{m}$ | mass flow | $kg \cdot s^{-1}$ |
| $n$ | number of electrons per mol $H_2$ ($n$ = 2) | --- |
| $\dot{n}$ | mole flow | $mol \cdot s^{-1}$ |
| $P_{el}$ | electric power | W |
| $p$ | pressure | Pa |
| $\dot{Q}_{trans}$ | exchanged heat | W |
| $R$ | general gas constant ($R$ = 8.31451) | $J \cdot mol^{-1} \cdot K^{-1}$ |
| $s$ | specific entropy of a stream | $J \cdot kg^{-1} \cdot K^{-1}$ |
| $T$ | temperature | K |
| $V$ | polarization voltage drop (overvoltage) | V |
| $w_{Fuel}$ | mass fraction of water in fuel | $kg \cdot kg^{-1}$ |
| $X_{Fuel}$ | fuel conversion rate | --- |
| $x$ | length coordinate in fuel cell channel | m |
| $y_i$ | molar fraction of species i | $mol \cdot mol^{-1}$ |

Greek symbols:

| | | |
|---|---|---|
| $\beta$ | exchange coefficient | --- |
| $\delta_k$ | thickness of layer k | m |
| $\eta$ | energetic efficiency | 1 |
| $\nu_i$ | stoichiometric coefficient of species i | --- |
| $\rho$ | specific electric resistance | $\Omega \cdot m$ |
| $\varphi_{SF}$ | steam/fuel ratio (total water to dry fuel) | $kg \cdot kg^{-1}$ |
| $\varphi_{bypass}$ | part of total air or fuel resp. in bypass | --- |

Subscripts:

| | |
|---|---|
| *AC* | alternate current |
| *a* | anode |
| *act* | activation polarization |
| *c* | cathode |
| *chem* | chemical |
| *conc* | concentration polarization |
| *cond* | condenser of steam or ORC cycle |
| *conv* | fuel conversion in the fuel cell stack |
| *DC* | direct current |
| *el* | electric |
| *exp* | effectively exported from the plant |
| *FC* | fuel cell |
| *FU* | fuel utilization (electricity and utilized heat) |
| *Fuel* | referring to biomass fuel |
| *G* | gasification |
| *HC* | hybrid cycle |
| *HRC* | heat recovery cycle |
| *i* | species in gas mixture or reaction |
| *in* | feed stream into the system |
| *inv* | inverter |
| *k* | component of the fuel cell |
| *net* | electric consumption subtracted |
| *ohm* | ohmic polarization |
| *out* | stream leaving the system |
| *Plant* | referring to the whole CHP plant |
| *Q, q* | heat |
| *r* | reversible operated fuel cell |
| *react* | actually reacting |
| *SG* | steam generation for fluidization |
| *vol* | voltage efficiency due to polarization |

## MODELING

### General aspects

Within the following, the term "modeling" largely refers to the energetic description of the process. The energetic performance is conventionally described in terms of energy based on LHV and sensible heat. The advantage of this method is the compatibility to common efficiency definitions. On the other hand, exergy may be used as the characteristic stream quality for process evaluation. According to Baehr [13], the exergy of a stream consists of the exergy of heat and chemical exergy. For ideal gas mixtures, the specific exergy is defined by:

$$e = e_q + e_{chem} \tag{1}$$

$$e_q = h(T) - h(T_0) - T_0 \cdot \left[ s(T,p) - s(T_0,p_0) \right] \tag{2}$$

$$e_{chem} = M^{-1} \cdot \left[ \sum_i \left( y_i \cdot E_{0i} \right) + R \cdot T_0 \cdot \sum_i \left( y_i \cdot \ln y_i \right) \right] \tag{3}$$

The thermal environment defined for the present study is 298.15 K, 0.1 MPa. Enthalpy and entropy in Eq. (2) are the properties of the gas mixture. While the pressure dependency of exergy is represented by the entropy term in Eq. (2), the entropy of mixing effect on exergy is not covered by Eq. (2). The reason is that the mixing entropy enters both entropy expressions in the square brake term of Eq. (2) in the same way. Therefore, the mixing irreversibility is part of the chemical exergy and represented by the right hand side addend in the square brake of Eq. (3). The molar exergy of pure substances at thermal environment conditions depends on the definition of a chemical environment. Baehr [13] reports the exergy at standard conditions (298.15 K, 0.1 MPa) for numerous chemical elements based on an equilibrium environment calculated by Diederichsen [14]. The standard exergy of chemical compounds can be calculated from element exergy and standard free enthalpy. For pure water and steam the exergy is defined by equations similar to Eqs. (1) and (2) using IAPWS-IF97 [15] data for temperature and pressure dependent enthalpy and entropy. Equation (3) reduces in the case of pure water to a constant. The exergy of solid mixtures is expressed in analogy to ideal gases with the simplification that the pressure dependency of entropy can be neglected. For organic mixtures defined just by elementary analysis, the entropy of formation is not available while the enthalpy of formation can be calculated from the heating value. The chemical exergy is set equal to the higher heating value for these substances, what should be a good approximation [16].

### Gasification and gas cleaning

As mentioned in the introduction, the modeling of the gasification process has been the subject of previous work and will not be described into detail here. The present work aims at an authentic representation of the gasification process taking measured plant data into account. The plant layout of the gasification and gas cleaning section is shown in Fig. 1. The gasifier is fluidized with superheated steam and the biomass fuel is introduced into the stationary bed using a screw feeding system. An important parameter is the total water to dry fuel ratio, in the following shortly called steam/fuel ratio:

$$\varphi_{SF} = \frac{\dot{m}_{Fuel} \cdot w_{Fuel} + \dot{m}_{Steam}}{\dot{m}_{Fuel} \cdot \left(1 - w_{Fuel}\right)} \tag{4}$$

The raw producer gas water content (27…48 v-%) strongly depends on the steam/fuel ratio, which takes values between 0.5 and 1.0 in practical operation.

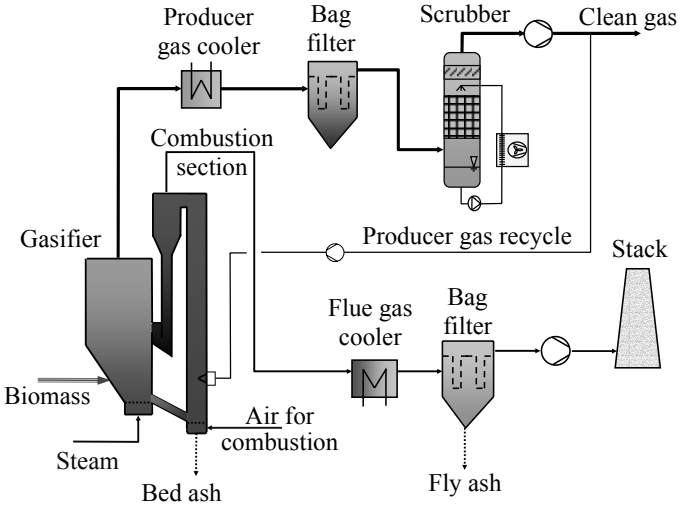


**Fig. 1: Layout of the Guessing steam gasification process.**

The temperature spread between combustion and gasification reactor is determined by the necessary energy for gasification and the bed material circulation rate. Further parameters with energetic significance are the amount of residual char that leaves the gasification section with the bed material and the gasification temperature. The pressure in both gasifier and combustion reactor is close to atmospheric conditions.

The gas conditioning section consists of producer gas cooler, bag filter, and a tar scrubber using rape oil methyl ester (RME) as solvent. The water content in clean producer gas is limited to the value for 100 % humidity at scrubber exit. Variation of the scrubber exit temperature (45…70 °C) results in clean gas water contents between 10 and 32 v-%. The condensate/RME solution is separated in an equalization tank and the water fraction is introduced in the hot flue gas line after part evaporation. A small part of the clean producer gas is recycled into the combustion reactor in order to control the gasification temperature. The bed material leaving the gasifier carries about 10 % of the dry fuel as residual char which is the main fuel for the combustion reactor. After leaving the fast fluidized bed combustor, the hot bed material is separated from flue gas in a cyclone and enters the gasifier through a steam-fluidized loop seal. After final heat recovery in the flue gas cooler, dust is separated in a bag filter while the gas goes to the stack.

For IRSOFC operation, all hydrocarbons except $CH_4$ must be eliminated from the producer gas because of the risk of carbon deposition on the fuel electrode [17]. The reforming can be realized inside the gasifier using catalytic active bed material or in a separate reforming unit directly after the gasifier. The present work assumes reforming of all higher hydrocarbons inside the gasifier. Measured data from the Guessing installation show, that the CO-shift reaction

$$CO + H_2O \leftrightarrow CO_2 + H_2 \qquad (5)$$

is very close to equilibrium at the exit of the gasifier. Therefore, the model assumes React. (5) to be in equilibrium at the gasifier exit. The $CH_4$ concentration is estimated based on the operating experience on different FICFB gasification systems.

Two efficiency values based on thermal fuel power describe the overall behavior of the gasification process. The chemical efficiency refers to the amount of energy combined in the exported producer gas:

$$\eta_{chem,G} = \frac{\dot{m}_{PG,\exp} \cdot lhv_{PG,clean}}{\sum\left(\dot{m}_{Fuel} \cdot lhv_{Fuel}\right)} \qquad (6)$$

The thermal efficiency of the gasification process relates the exportable heat, which is the heat transferred in producer gas cooler and flue gas cooler reduced by the heat needed for steam generation, to the primary fuel power:

$$\eta_{Q,G} = \frac{\dot{Q}_{trans,PG-cooler} + \dot{Q}_{trans,FG-cooler} - \sum \dot{Q}_{trans,SG}}{\sum\left(\dot{m}_{Fuel} \cdot lhv_{Fuel}\right)} \qquad (7)$$

The aim of the optimization of the gasification process is a high chemical efficiency. The influence of additional biomass fuel to the combustion chamber on the chemical efficiency will be discussed in the results section.

## Internal reforming solid oxide fuel cell (IRSOFC)

Solid oxide fuel cells typically work at temperatures between 800 and 1000 °C. The electrolyte is normally an ion-conducting $ZrO_2$-$Y_2O_3$ solid solution with an $Y_2O_3$ content of 8-10 mol-%. The porous electrodes are electron conducting. The anode (fuel electrode) material is a cermet of Ni and $ZrO_2$, a largely applied cathode (air electrode) material is Sr-doped $LaMnO_3$. Different SOFC developers present either tubular or planar cell design. The electrochemical reaction taking place at the three-phase boundary fuel/anode/electrolyte is:

$$H_2 + O^{2-} \rightarrow H_2O + 2e^- \qquad (8)$$

On the cathode side, oxygen is electrochemically reduced to oxygen ions which are actually transported in the electrolyte:

$$\tfrac{1}{2}O_2 + 2e^- \rightarrow O^{2-} \qquad (9)$$

The overall oxidation reaction is therefore:

$$H_2 + \tfrac{1}{2}O_2 \rightarrow H_2O \qquad (10)$$

At the operating temperatures of the SOFC, a direct electrochemical oxidation of CO at the anode/electrolyte boundary would be theoretically possible. However, the CO-shift reaction (React. 5) is kinetically faster and the equilibrium is driven to the right by the hydrogen consume of React. (10). The anode is as well a catalyst for steam reforming of $CH_4$ according to

$$CH_4 + 2\,H_2O \rightarrow CO_2 + 4\,H_2\,. \qquad (11)$$

The equilibrium of React. (11) is far on the right at the operating conditions of the SOFC, kinetic inhibition is the only reason for possible incomplete conversion. In analogy with the literature [4], the present work assumes that $CH_4$ is completely reformed when passing the anode. In order to prevent solid carbon deposition on the anode surface, the molar steam to combustible carbon ratio (S/C ratio) in the anode feed must be high enough. Typical values for the S/C ratio in order to effectively avoid carbon deposition are 3.0-3.5 [18]. Incomplete fuel conversion is expressed in terms of CO and $H_2$ passing by. Reaction (5) is assumed to be in equilibrium in the anode exhaust.

In order to investigate the combination of the existing gasification process and fuel cell technology for power generation, a model has been developed taking the energetic behavior of the fuel cell stack into account. To allow direct comparison to other power generation units like gas turbine or engine, the basis for the efficiency formulation is the thermal fuel power of the anode feed based on LHV. The overall electric efficiency of the cell stack including the DC/AC inverter is:

$$\eta_{el,FC} = \frac{P_{el,AC}}{\dot{m}_{a,in} \cdot lhv_{a,in}} \qquad (12)$$

The overall efficiency is a product of reversible cell efficiency, voltage efficiency, fuel conversion efficiency, and inverter efficiency:

$$\eta_{el,FC} = \eta_r \cdot \eta_{vol} \cdot \eta_{conv} \cdot \eta_{inv} \qquad (13)$$

The reversible cell efficiency used within the present work largely corresponds to the commonly used thermodynamic efficiency, which is an upper bound for the fuel cell efficiency comparable to the Carnot cycle efficiency for heat engines. The reversible cell efficiency relates the open circuit voltage at operating conditions to the theoretical cell potential if the enthalpy of formation of gaseous $H_2O$ at 298.15 K would account for the voltage:

$$\eta_r = \frac{E_r}{E_0} \qquad (14)$$

This definition is compatible to efficiency definitions for engines based on the LHV of the fuel gas. The open circuit voltage depends on temperature and on the partial pressures of the gas species in React. (10). The present work presumes a constant cell stack temperature. The gas composition, however,

changes along the fuel cell channel. The reversible cell potential for changing partial pressures is generally given by:

$$E_r = \frac{-\Delta G_R^0(T)}{n \cdot F} - \frac{1}{L} \cdot \int_{x=0}^{L} R \cdot T \cdot \ln\left( \prod_i p_i^{-\nu_i}(x) \right) \cdot dx \quad (15)$$

For means of simplification, the concentration changes are assumed to be linear between gas feed and drain on both anode and cathode side. The analytical solution of Eq. (15) is then [3]:

$$E_r = \frac{-\Delta G_R^0(T)}{n \cdot F} + \\ + R \cdot T \cdot \sum_i \left\{ \nu_i \cdot \left[ \frac{p_{i,in}}{p_{i,out} - p_{i,in}} \cdot \ln\left( \frac{p_{i,out}}{p_{i,in}} \right) + \ln\left( p_{i,out} \right) + 1 \right] \right\} \quad (16)$$

The theoretical potential that corresponds to the enthalpy of formation of gaseous $H_2O$ at 298.15 K is a constant:

$$E_0 = \frac{-\Delta_f H_{298}^0(H_2O(g))}{n \cdot F} = 1.253 \text{ V} \quad (17)$$

If current is drawn from the fuel cell, the voltage decreases with increasing current density due to irreversibility in the different parts of the cell. This voltage drop is termed polarization or overvoltage. Most authors divide the polarization effect in activation overvoltage, ohmic loss, and concentration overvoltage. The activation polarization can be described by the Butler-Volmer equation according to:

$$\frac{i}{i_0(T)} = \exp\left( \frac{\beta \cdot F \cdot V_{act}}{R \cdot T} \right) - \exp\left( -\frac{(1-\beta) \cdot F \cdot V_{act}}{R \cdot T} \right) \quad (18)$$

The exchange coefficient is assumed to be 0.5 for the fuel cell application [12]. The exchange current density is proportional to the forward and reverse reaction rate at stack temperature. The temperature dependency of $i_0$ is described by an Arrhenius approach:

$$i_0(T) = i_{00} \cdot \exp\left( -\frac{E_{A,i_0}}{R \cdot T} \right) \quad (19)$$

The constants in Eq. (19) could be obtained from data reported by Chan et al. [8] for a tubular IRSOFC (Siemens Westinghouse Design) as $i_{00}$ = 71960 A·m$^{-1}$ and $E_{A,i0}$ = 48.76 kJ·mol$^{-1}$. If data is available, the activation can be expressed separately for each electrode. The ohmic polarization is determined by the resistance of the ion conducting electrolyte and the electron conducting electrodes and interconnections. The voltage drop for constant effective area (e.g. planar cell) is:

$$V_{ohm} = i \cdot \sum_k \left( \rho_k \cdot \delta_k \right) \quad (20)$$

In the case of tubular cells, the current density changes in the radial direction must be considered. For the temperature dependency of ionic conduction, the following correlation is reported in the literature [19]:

$$\frac{1}{\rho(T)} = \frac{A_{ohm}}{T} \cdot \exp\left( -\frac{E_{A,ohm}}{R \cdot T} \right) \quad (21)$$

Data from the literature [9] has been used to determine the constants in Eq. (21) describing the overall ohmic resistance of the tubular fuel cell mentioned above for an estimated thickness $\delta$ of 6.16·10$^{-4}$ m: $A_{ohm}$ = 8.5·10$^6$ and $E_{A,ohm}$ = 52.4 kJ·mol$^{-1}$. Concentration overvoltage occurs due to the decreasing partial pressure of the reactants at the three phase boundaries because of limited diffusion in the electrodes. Complex polarization models have been developed by Chan et al. [12]. Within the present work, a simplified description according to Chan et al. [8] is applied:

$$V_{conc} = -\frac{R \cdot T}{n \cdot F} \cdot \ln\left( 1 - \frac{i}{i_L(T)} \right) \quad (22)$$

Concentration polarization is not significant if the cell stack is operated well below the limiting current density, which again is a function of operating temperature. The temperature dependency is expressed by the simple correlation

$$i_L(T) = a_{i_L} + b_{i_L} \cdot T \quad (23)$$

The coefficients have been fit from literature data [9] for the tubular IRSOFC: $a_{iL}$ = 1750 A·m$^{-2}$, $b_{iL}$ = 5.65 A·m$^{-2}$·K$^{-1}$. The actual cell voltage at a certain current density is:

$$E = E_r - \sum V \quad (24)$$

The voltage efficiency of the charged cell is therefore:

$$\eta_{vol} = \frac{E}{E_r} \quad (25)$$

In a real SOFC, the fuel will never be completely converted. Therefore, a conversion efficiency of the cell stack can be generally defined as

$$\eta_{conv} = \frac{\dot{n}_{H_2,react} \cdot LHV_{H_2}}{\dot{m}_{a,in} \cdot lhv_{a,in}} \quad (26)$$

The amount of actually reacting hydrogen can be related to the total current of the cell stack:

$$\dot{n}_{H_2,react} \cdot LHV_{H_2} = \frac{i \cdot A_{eff}}{n \cdot F} \cdot \left[ -\Delta_f H_{298}^0(H_2O(g)) \right] \quad (27)$$

It is important to notice that the conversion efficiency defined by Eq. (26) implies the energetic effects of possible fuel conversions like reforming and shifting. In the case of high rates of endothermic reforming, the conversion efficiency can take values above unity even though $H_2$ and CO may be left in the exhaust. In this case, a part of the heat produced by

polarization is recombined into the fuel by the reforming reaction. The total fuel conversion rate often used in the literature is defined for the IRSOFC in terms of $H_2$ equivalents. According to React. (5) and (11), one mole of CO equals one mole of $H_2$, while one mole of $CH_4$ equals 4 moles of $H_2$. The overall fuel conversion rate can be written as:

$$X_{Fuel} = 1 - \frac{\dot{n}_{a,out} \cdot \sum\left(y_{H_2,equiv.,a,out}\right)}{\dot{n}_{a,in} \cdot \sum\left(y_{H_2,equiv.,a,in}\right)} \qquad (28)$$

For pure hydrogen as fuel, $\eta_{conv}$ is equal to $X_{fuel}$.

Finally, the efficiency of the DC/AC inverter, defined as

$$\eta_{inv} = \frac{P_{el,AC}}{P_{el,DC}} \qquad (29)$$

must be considered. $\eta_{inv}$ is set to 96.5 % for the present work.

## SOFC-GT hybrid process

Massardo et al. [4] present four basic options for the layout of a SOFC-GT cycle with heat recovery steam generation. One of these concepts has been further investigated by Chan et al. [8,9] who also focus on part load behavior [10]. The process set up discussed in the present work is based on these sources. However, the final heat recovery from exhaust gas is left to a further process downstream of the hybrid cycle section. The scheme of the fuel cell-GT section is shown in Fig. 2.

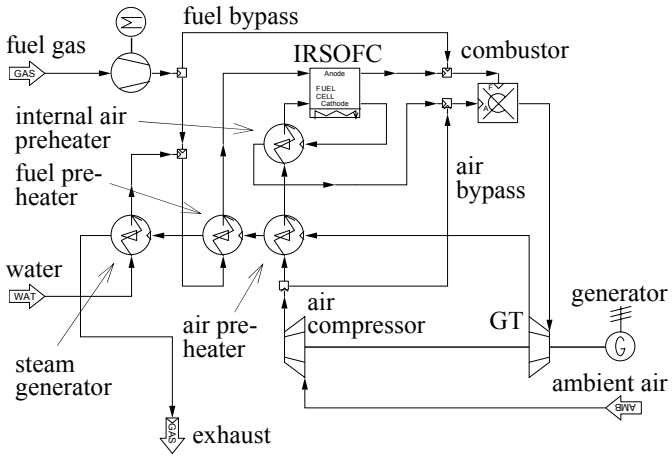


**Fig. 2: IRSOFC-GT hybrid process.**

Additional steam to the fuel gas may be necessary in order to reach the S/C ratio required for preventing carbon deposition on the electrode. The fuel cell stack is modeled isotherm and adiabatic. Heat produced due to dissipation is therefore affecting the temperature inside the IRSOFC stack. In contrast to natural gas fuelled cells, the heat consumption by endothermic reforming is low for producer gas, which may require adoption of the cell design in order to use the incoming gas streams to cool the cell stack. The two exhaust streams of the fuel cell are mixed in a combustion chamber, where complete combustion of the fuel is assumed. The fuel bypass around the fuel cell is used during start-up and for control purposes. The air bypass allows the limitation of the turbine inlet temperature (TIT). The GT is described by its isentropic efficiency. The air compressor is directly coupled to the GT, while the fuel compressor is electric powered. With respect to practical operating stability, Chan et. al. [8,10] suggest a set up with two GT, one to drive the air compressor and a power turbine coupled to the generator. The present work focuses on energetic behavior. Therefore, the simpler concept with just one GT has been taken into consideration. The turbine exhaust is used to preheat both air and fuel stream and for anode steam generation before leaving the section towards heat recovery.

## Heat recovery cycle (HRC)

The exhaust temperature of the hybrid cycle is typically about 400 °C. Producer gas and flue gas cooling in the gasification section also provides a considerable amount of high level heat. Steam cycle and ORC have been investigated as possible heat recovery concepts. Electrical efficiencies are summarized in Table 2. The steam parameters are 450 °C/8.2 MPa/450 °C/2.0 MPa for the 2-stage cycle, 450 °C/1.8 MPa for the 1-stage cycle. Steam turbine isentropic efficiency is 80 %. For the ORC, the hot side temperature level is 280 °C and the ratio $\eta_{el}/\eta_{Carnot} = 0.4$.

**Table 2**
**Heat-to-electricity efficiency for steam cycle and ORC at different condensation temperatures.**

| | $\eta_{el}$ [%] | $T_{cond}$ [°C] | $p_{cond}$ [MPa] |
|---|---|---|---|
| 1-stage steam cycle | 16…25 | 120…40 | 0.2…0.008 |
| 2-stage steam cycle | 20…32 | 120…40 | 0.2…0.008 |
| ORC | 12…18 | 120…40 | --- |

## RESULTS AND DISCUSSION

## Gasification section

The input parameters for the simulation are derived from data measured at the Guessing plant. The water content of the biomass fuel is 20 wt.-% and the LHV is 13.97 MJ·kg$^{-1}$. The gasifier is operated at 850 °C and a steam/fuel ratio of 0.75. The concentration of $CH_4$ after the integrated reforming step is set conservatively to 10.0 v-%(dry). The resulting producer gas composition is specified in Table 3. The tar scrubber is operated at 65 °C, what results in a clean gas water content of 25.7 v-%.

**Table 3**
**Producer gas composition from FICFB steam gasification at 850 °C including pre-reforming**

| | | |
|---|---|---|
| $CH_4$ | v-% (dry) | 10.0 |
| CO | v-% (dry) | 21.6 |
| $CO_2$ | v-% (dry) | 21.2 |
| $H_2$ | v-% (dry) | 45.8 |
| $N_2$ | v-% (dry) | 1.4 |
| LHV | MJ/m$^3_N$ (dry) | 11.3 |
| $H_2O$ | v-% | 33.3 |

The calculated energetic data of the gasification and gas cleaning section are summarized in Table 4 for a total fuel power of 8.0 MW. Further improvement of the gasification process might be reached by lowering the gasification temperature or by integrated fuel drying. However, these aspects are beyond the focus of this study.

**Table 4**
**Energetic performance of the 8 MW steam gasification process.**

| | | |
|---|---|---|
| Fuel | kW | 8000 |
| Heat producer gas cooler | kW | 920 |
| Heat flue gas cooler | kW | 626 |
| Total heat steam generation | kW | 529 |
| Power of exported PG | kW | 5788 |
| Electric power input | kW | 50 |
| $\eta_{chem}$ | % | 72.4 |
| $\eta_{Q,G}$ | % | 12.7 |

## IRSOFC performance

The energetic performance of the IRSOFC stack is investigated for producer gas with a dry composition according to Table 3 and a water content of 53 %. The S/C ratio of the fuel mixture is 3.5. In the design of cell stacks, effective cooling by an adequate air distribution is a key issue. Within the present work the cell stack is modeled isothermal and the air utilization is set to 25 % (15.3 v-% $O_2$ in the cathode exhaust). The heat balance for operation at 1000 °C/2000 A·m$^{-2}$ is fulfilled with anode feed preheated to 650 °C and cathode feed to 696 °C.

From all factors determining the total electric efficiency of the fuel cell according to Eq. (13), only polarization is depending on current density. Therefore, the efficiency is presented together with the effective voltage in Fig. 3 for a certain fuel utilization and stack pressure. Figure 4 shows the power density of the cell on current density. The working point must be fixed according to economic aspects regarding stack size and stack efficiency. To assure operation stability, the actual current density should be to the left of the power density peak.

The pressure impact on cell voltage and electric efficiency is shown in Fig. 5. Note that the x-axis shows absolute pressure and atmospheric pressure is therefore at 0.1 MPa. Polarization efficiency increases together with the reversible cell voltage because the voltage drop due to polarization remains constant.

## SOFC-GT hybrid cycle

The hybrid cycle shown in Fig. 2 is fuelled with clean producer gas. The water content in anode feed is increased from 26 v-% to 53 v-% by injection of steam after producer gas compression. The settings for the simulation of the hybrid cycle are summarized in Table 5. The fuel utilization is 85 % in the fuel cell and 100 % in the combustor. The fuel bypass indicated in Fig. 2 is zero for standard operation while the air bypass follows the required turbine inlet temperature (TIT). The power for fuel compression must be subtracted from the brut power produced.

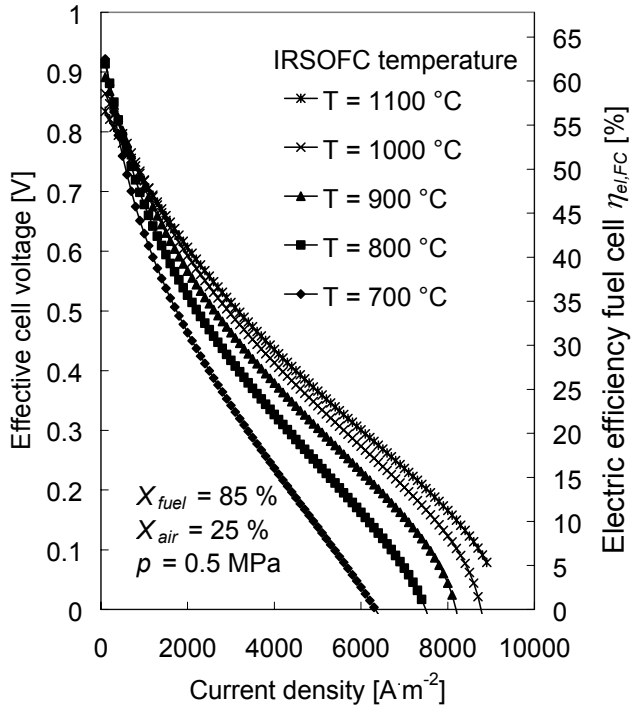


**Fig. 3: Effective voltage and electric efficiency of the fuel cell vs. current density.**

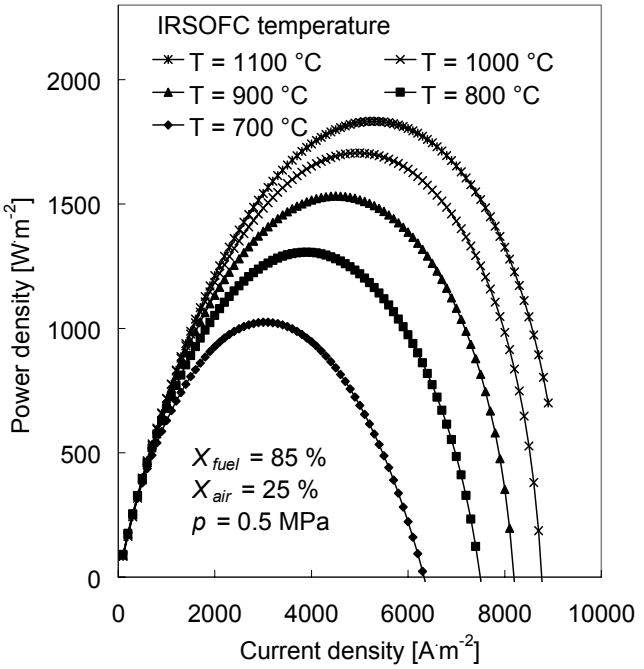


**Fig. 4: Power density of the fuel cell vs. current density.**

The energetic potential of the exhaust is described by $\eta_{Q,HC}$ as the transferred heat if the gas were cooled to a stack temperature of 150 °C. The performance of the hybrid cycle

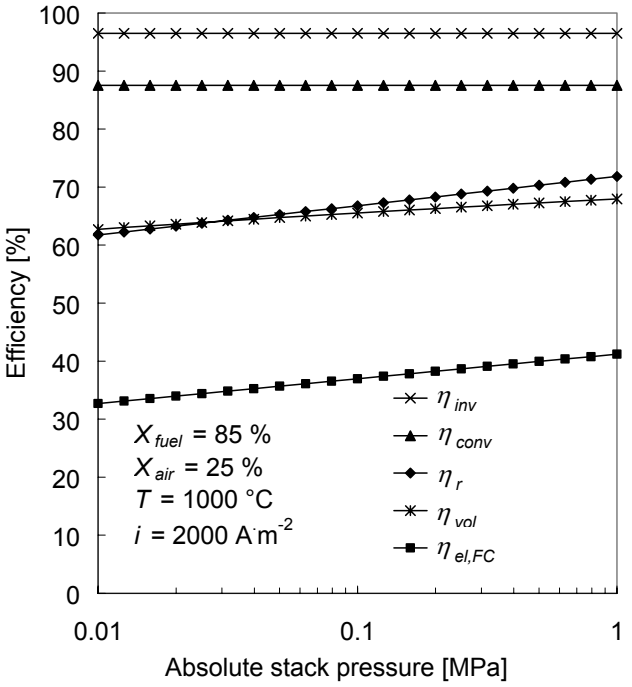


**Fig. 5: Fuel cell performance vs. stack pressure.**

versus operating pressure in Fig. 6 shows a flat maximum electric efficiency between 0.6 and 0.9 MPa, which may be shifted to right if the air compression would include interstage coolers. The behavior is dominated by the GT cycle characteristics, where the TIT is set to 900 °C. At 0.9 MPa the air bypass approaches zero and fuel must be bypassed in order to reach the TIT.

In order to reach high electric efficiencies in stable operation and at bearable investment costs, the practical working point will be left to the peak in Fig. 6. The heat efficiency shows, how much of the thermal power input to the hybrid cycle can be used by a HRC cooling the exhaust stream to 150 °C.

## Plant performance including heat integration

The hybrid cycle is coupled to the gasification process by using the exported producer gas as fuel. In order to increase the plant electric efficiency, a heat recovery concept that covers both hybrid cycle exhaust enthalpy and the net cooling energy from the gasification process is considered. The performance of different technologies has already been presented in the modeling section. In the practical implementation of a steam cycle concept, the whole line of preheating, evaporation, and superheating must be implemented separately for GT exhaust and flue gas unless the flue gas filter and blower operate at heat recovery inlet temperature (550 °C). The heat for the generation of fluidization steam must be decoupled from the steam cycle. If an ORC is used for heat recovery, heat carrier oil is used to bring the energy from the coolers to the actual Rankine cycle. In this case, fluidization steam generation can also be powered by the heat carrier oil.

**Table 5**
**Parameters in the simulation of the SOFC-GT hybrid cycle shown in Fig. 2.**

| | |
|---|---|
| Pressures [MPa]: | |
| ambient air | 0.101 |
| clean producer gas | 0.097 |
| anode and cathode feed | 0.15…1.20 |
| turbine exhaust | 0.105 |
| Temperatures [°C]: | |
| ambient air | 15 |
| clean producer gas | 65 |
| fuel cell inlet anode side | 392* |
| air feed to internal air preheater | 472* |
| fuel cell inlet cathode side | 771* |
| fuel cell exhaust anode side | 1000 |
| fuel cell exhaust cathode to internal preheater | 1000 |
| cathode exhaust after internal preheater | 691* |
| turbine inlet temperature (TIT) | 900 |
| Pressure drops [%]: | |
| fuel preheater (fuel/exhaust) | 1 / 1 |
| air preheater (air/exhaust) | 1 / 1 |
| fuel cell stack anode side | 2 |
| cathode side incl. internal air preheater | 3 |
| combustor (anode exhaust/cathode exhaust) | 2 / 2 |
| Efficiencies [%]: | |
| fuel compressor (isentropic/shaft/motor) | 80 / 99 / 96 |
| air compressor (isentropic/shaft) | 80 / 99 |
| gas turbine (isentropic/shaft/generator) | 80 / 99 / 97 |

*) Temperatures changing with pressure/load due to constant heat exchanger area, values for 0.5 MPa cell stack pressure.

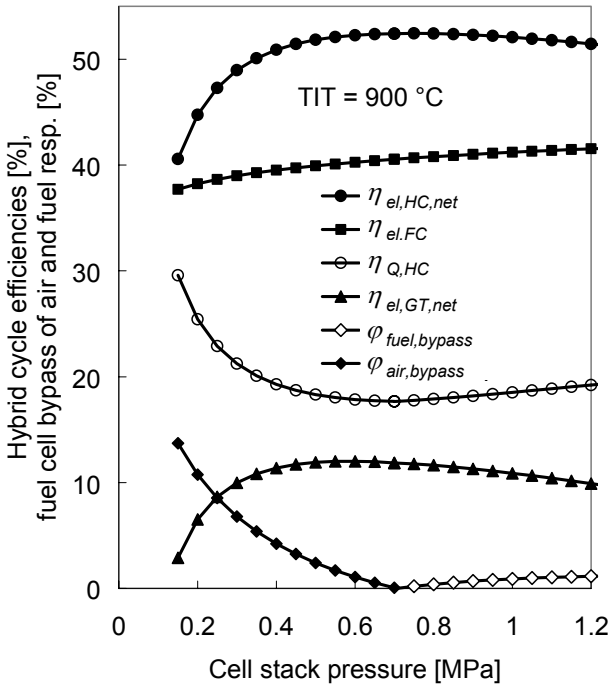


**Fig. 6: Hybrid cycle performance vs. fuel cell operating pressure with a TIT limit set to 900 °C.**

The plant electric efficiency is:

$$\eta_{el,Plant} = \frac{\sum P_{el,produced} - \sum P_{el,consumed}}{\sum \left( \dot{m}_{fuel} \cdot lhv_{fuel} \right)} \qquad (30)$$

The heat efficiency in the case of CHP operation is given by:

$$\eta_{Q,Plant} = \left( \eta_{chem,G} \cdot \eta_{Q,HC} + \eta_{Q,G} \right) \cdot \eta_{Q,HRC} \qquad (31)$$

If the cooling temperature of the HRC is such that no heat can be exported, $\eta_{Q,HRC}$ becomes zero. In the case of the one or two stage steam cycle there is still the heat from producer gas cooling (with the evaporation energy for scrubber condensate and fluidization steam subtracted) available for heat export.

The plant performance for the three different heat recovery concepts is summarized in Table 6. The gas generation is operated according to Table 4, the hybrid cycle parameters are those of Table 5 with 0.5 MPa fuel cell operating pressure. The heat recovery cycles behave according to Table 2. Producer gas, flue gas, and GT exhaust are cooled to 150 °C.

**Table 6**
**Plant efficiency data calculated for different heat recovery technologies.**

| Concept | $T_{Q,exp}$ [°C] | $\eta_{el,HRC}$ [%] | $\eta_{Q,HRC}$ [%] | $\eta_{el,Plant}$ [%] | $\eta_{Q,Plant}$ [%] | $\eta_{FU,Plant}$ [%] |
|---|---|---|---|---|---|---|
| 1-stage steam cycle | 40 | 25.4 | --- | 43.5 | --- | 43.5 |
| | 120 | 15.7 | 83.6 | 41.0 | 21.7 | 62.7 |
| 2-stage steam cycle | 40 | 31.3 | --- | 45.0 | --- | 45.0 |
| | 120 | 22.6 | 76.5 | 42.8 | 19.9 | 62.6 |
| ORC | 40 | 17.4 | --- | 41.4 | --- | 41.4 |
| | 120 | 11.8 | 87.2 | 40.0 | 22.6 | 62.6 |

For the rather complex concept with a two stage steam cycle and a condensation turbine, the plant reaches an electric efficiency of 45 %. Economically, such a configuration may be of interest for installations above 100 MW fuel power. The difference in efficiency to the one stage steam cycle of only two percentage points may be outweighed by economic aspects. Since compact ORC units are available on the market, this technology allows a simple plant configuration. For CHP in the capacity range below 20 MW fuel power, the ORC concept is probably the most promising from the economic point of view. The energy consumption by steam generation for both gasifier fluidization and anode feed humidification results in rather low global efficiency values of only about 62 % in CHP operation.

## Optimization potential and exergy

Any optimization approach has to take the ratio between possible improvement in efficiency and related costs into account. The theoretical potential for improvement of a certain process unit is quantified by its exergy loss. To get a more practical approach towards the optimization potential, the irreversibilities must be divided into avoidable and unavoidable losses [3]. In order to emphasize the different quality of different forms of energy like electricity, chemical combined energy, and sensible heat, the exergetic behavior is shown in Fig. 7 for a typical CHP operation using an ORC for heat recovery. The exergy of the streams is defined by Eqs. (1)-(3) and electricity is considered pure exergy.

The main exergy loss can be found in the gasification section. These losses are practically not avoidable due to the irreversible nature of high temperature reactions far from chemical equilibrium (i.e. gasification, combustion). Improvement is possible by operation at lower gasification temperatures and at higher bed material circulation rates (lower temperature difference between gasification and combustion reactor). The loss in gas cleaning is relatively high due to the cooling of the scrubber solvent to the environment. The loss due to producer gas cooling is practically not avoidable because low gas temperatures are required for the fuel compressor.

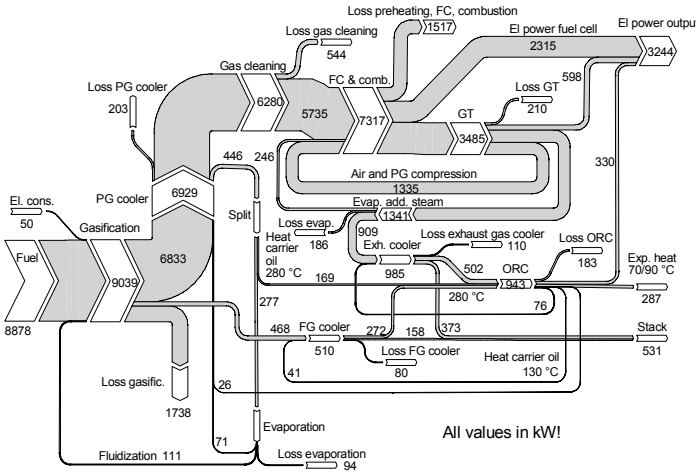


**Figure 7. Exergy streams of a CHP plant with an ORC for heat recovery (ambient air and liquid water exergy omitted).**

The exergy loss of the fuel cell including feed compression, feed preheating, and post combustion of the exhaust is partly avoidable as far as the polarization losses in the fuel cell are concerned. However, the polarization exergy loss is only about 424 kW, 84 kW are lost in the DC/AC inverter for the efficiency chosen. Polarization decreases with increasing stack area. An optimum has to be chosen according to economics. Another critical point with respect to plant efficiency is the high amount of steam added to the anode feed. If the IRSOFC can be operated at a lower S/C ratio, the reversible cell potential increases and the energy consumption for steam generation decreases. The main part of the electricity is produced in the hybrid cycle while the HRC contributes only with about 10 % to the total electricity production. It is obvious, that the HRC efficiency influences the plant performance only marginally and rather the cheapest than the most efficient HRC concept should be selected. Summarizing, the greatest potential for short-term optimization of the process can be located in the gasification section and in fuel cell operation at a reduced S/C ratio. On a long term basis, rigorous changes in the operation mode like pressurized gasification in combination with hot producer gas cleaning can lead to significant improvement of the energetic performance.

## CONCLUSIONS

The energetic potential of a coupling between biomass steam gasification and an SOFC-GT hybrid cycle is investigated. Therefore, an energetic model of an IRSOFC stack has been developed based on data from the literature. The characteristic behavior of the fuel cell presented agrees well with other models [8,9]. For the gasification and gas cleaning section, measured data from the 8 MW fuel power commercial plant in Guessing/Austria are considered. The chemical efficiency of the gasifier reaches 72.4 % based on LHV for a fuel water content of 20 wt.-%. The simulation results for three different concepts of heat recovery are presented: one and two stage steam cycle and a compact ORC unit. The whole plant is implemented in the process simulation tool IPSEpro. The plant electric efficiencies with heat recovery are 40-43 % for CHP operation depending on the HRC technology. For a 2-stage steam cycle in condensation operation as HRC, 45 % electric efficiency may be reached. The largest exergy losses occur in the gasification section. Cell polarization, feed preheating and exhaust combustion cause the main exergy loss of the hybrid cycle. Significant short-term improvement of the process can therefore be reached by reducing the irreversibilities during gas generation. Higher fuel and air utilization rates and a lower S/C ratio in the SOFC also result in a better plant performance. The HRC contributes only marginally to the total electricity output. The choice, which HRC concept can be economically realized depends therefore strongly on the capacity of the plant. Further work will aim at the installation of an SOFC test unit in a side stream of the Guessing plant.


## ACKNOWLEDGMENT

The authors gratefully acknowledge financial support from the Austrian funds program "Knet".


## REFERENCES


[1] Hofbauer, H., Rauch, R., Loeffler, G., Kaiser, S., Fercher, E., and Tremmel, H., 2002, "Six Years Experience with the FICFB-Gasification Process", Proc., 12th European Biomass Conference, W. Palz et al., eds., ETA, Florence, Italy, pp. 982-985.

[2] Hofbauer, H., Rauch, R., Bosch, K., Koch, R., Aichernig, C., 2003, "Biomass CHP plant Guessing – a success story", In: Pyrolysis and Gasification of Biomass and Waste, Bridgwater, A.V., Ed., CPL Press, Newbury, UK, pp. 527-536.

[3] Kaiser, S., 2001, "Simulation und Modellierung von KWK-Verfahren auf Basis Biomassvergasung", Ph.D. thesis, Vienna University of Technology, Austria.

[4] Massardo, A.F., Magistri, L., 2000, "Internal Reforming Solid Oxide Fuel Cell-Gas Turbine Combined Cycles (IRSOFC-GT): Part A- Cell Model and Cycle Thermodynamic Analysis", ASME J. Eng. Gas Turbines Power, **122**, pp. 27-35.

[5] Campanari, S., 2000, "Full Load and Part-Load Performance Prediction for Integrated SOFC and Microturbine Systems", ASME J. Eng. Gas Turbines Power, **122**, pp. 239-246.

[6] Magistri, L., Costamagna, P., Massardo, A.F., Rodgers, C., McDonald, C. F., 2002, "A Hybrid System Based on a Personal Turbine (5 kW) and a Solid Oxide Fuel Cell Stack: A Flexible and High Efficiency Energy Concept for the Distributed Power Market", ASME J. Eng. Gas Turbines Power, **124**, pp. 850-857.

[7] Selimovic, A., Palsson, J., "Networked solid oxide fuel cell stacks combined with a gas turbine cycle", J. Power Sources, **106**, pp. 76-82.

[8] Chan, S.H., Ho, H.K., Tian, Y., 2002, "Modelling of simple hybrid solid oxide fuel cell and gas turbine power plant", J. Power Sources, **109**, pp. 111-120.

[9] Chan, S.H., Ho, H.K., Tian, Y., 2003, "Multi-level modeling of SOFC-gas turbine hybrid system", Int. J. Hydrogen Energy, **28**, pp. 889-900.

[10] Chan, S.H., Ho, H.K., Tian, Y., 2003, "Modelling for part-load operation of solid oxide fuel cell-gas turbine hybrid power plant", J. Power Sources, **114**, pp. 213-227.

[11] Andries, J., Buhre, B.J.P., 2000, "Small-scale, distributed generation of electricity and heat using integrated biomass gasification-gas turbine-fuel cell systems", DGMK Tagungsber, 2000-1, pp. 115-125.

[12] Chan, S.H., Khor, K.A., Xia, Z.T., 2001, "A complete polarization model of a solid oxide fuel cell and its sensitivity to the change of cell component thickness", J. Power Sources, **93**, pp. 130-140.

[13] Baehr, H.D, 2000, Thermodynamik, Springer, Berlin.

[14] Diederichsen, Ch., 1991, "Referenzumgebungen zur Berechnung der chemischen Exergie", Fortschritt-Ber. VDI, Reihe 19, Nr. 50, VDI-Verlag, Duesseldorf, Germany.

[15] The International Association for the Properties of Water and Steam, 1997, "Release on the IAPWS Industrial Formulation 1997 for the Thermodynamic Properties of Water and Steam", Erlangen, Germany.

[16] Baehr, H.D., 1979, "Die Exergie der Brennstoffe", Brennst.-Waerme-Kraft, **31**, pp. 292-297.

[17] Eguchi, K., Kojo, H., Takeguchi, T., Kikuchi, R., Sasaki, K., 2002, "Fuel flexibility in power generation by solid oxide fuel cells", Solid State Ionics, **152-153**, pp. 411-416.

[18] Twigg, M.V., 1989, Catalyst Handbook, 2nd Ed., Wolfe Publishing Ltd., London, UK.

[19] Pimenov, A., Ullrich, J., Lunkenheimer, P., Loidl, A., Ruescher, C.H., 1998, "Ionic conductivity and relaxations in $ZrO_2$-$Y_2O_3$ solid solutions", Solid State Ionics, **109**, pp. 111-118.